FOREWORD

The research work in this report was performed by Aerojet-General Corporation, Azusa, California, for the Flight Dynamics Laboratory, Directorate of Aeromechanics, Deputy Commander/Technology, Aeronautical Systems Division, Wright-Patterson Air Force Base, under AF Contract Nr. AF33(616)-7420. This research is part of a continuing effort to advance the aeroelastic state-of-the-art knowledge for flight vehicles which is part of the Air Force Systems Command's Applied Research Program 750A, the Mechanics of Flight. The Project Nr. is 1370, "Dynamic Problems in Flight Vehicles", and the Task Nr. is 137003, "Prediction Methods for Dynamic Instabilities and Related Gasdynamic Phenomena". Thor M. Snaring, 1st Lt., USAF, of the Flight Dynamics Laboratory was the Project Engineer. The research was conducted from June 1960 to April 1962 by the Technical Staff of the Spacecraft Division.

This is the fourth of several reports to be published under AF Contract AF33(616)-7420. The previous reports (ASD-TDR-62-44; -155, Pt I; -294, Pt I) cover various other aspects of the investigation under this contract. The contractor's report number for the present report is 2214.

Bernard Mazelsky, consultant, is the principal investigator for the research activity of Aerojet-General Corporation. Although the studies were a group effort, the chief contributors were Bernard Mazelsky and Harry B. Amey, Jr.

ABSTRACT

A method is described for obtaining generalized aerodynamic forces by utilizing the NASA Kernel-Function Procedures. An evaluation of the generalized aerodynamic forces and the consequent flutter conditions is made for the particular case of a uniform, cantilevered, 70° delta wing. The supersonic Kernel-Function Procedure was found to be inadequate for treating the elastic modes on this low-aspect-ratio wing; the subsonic procedure, however, appears to work satisfactorily.

The theoretical flutter predictions are compared with the experimental results of NASA Report TM X-53. The Kernel-Function predictions for quasi-steady flow ($k \to 0$) appear to be superior to those for the complete unsteady case $\left(k = \frac{\omega_f c_r}{2V_f}\right)$. Based on this limited comparison, it appears that for this low-aspect-ratio wing the large transient effects predicted by linearized theory in the transonic regime may not actually exist.

PUBLICATION REVIEW

This report has been reviewed and is approved.

FOR THE COMMANDER:

AMBROSE B. NUTT
Asst. Chief, Dynamics Branch
Flight Dynamics Laboratory

TABLE OF CONTENTS

LIST OF SYMBOLS

ω_1, ω_2, ω_f	Vibration and flutter frequency of wing
V	Velocity of wing; subscript, f, denotes velocity of flutter
h_i	Amplitude of motion of the ith vibration mode
ρ	Density of airstream
S	Wing area
t	Time
A	Wing aspect ratio
C_{L_α}	Lift-curve slope
$\bar{\lambda}$	Taper ratio of wing
Λ	Leading-edge sweep angle
$\hat{Q}_{ij}$	Generalized aerodynamic force
Q_{ij}	Normalized generalized force
$Q_{\alpha_{ij}}$	Normalized generalized force due to $\partial h/\partial x$
$Q_{h_{ij}}$	Normalized generalized force due to h
$Q_{\Theta_{ij}}$	Normalized generalized force due to both h and $\partial h/\partial x$
$\bar{m}$	Generalized mass
$\bar{Q}_{ij}$	Ratio of generalized force to mass
$\bar{Q}_{R_{ij}}$, $\bar{Q}_{I_{ij}}$	Real and imaginary part of $\bar{Q}_{ij}$
w_j	Downwash of the jth vibration mode
$\bar{x}$, $\bar{\xi}$	Chordwise coordinates of wing (see Fig. 1)
$\bar{y}$, $\bar{\eta}$	Spanwise coordinates of wing

LIST OF SYMBOLS (cont.)

c_r	Root chord
b_o, b	Root semichord in subsonic and supersonic flow respectively
ℓ, 2bs	Semispan of wing in subsonic and supersonic flow respectively
x, ξ	Nondimensional chordwise coordinate, referenced to b_o and 2b in subsonic and supersonic flow respectively
y, η	Nondimensional spanwise coordinate, referenced to ℓ and 2b in subsonic and supersonic flow respectively
θ	Angular chordwise variable (see Eq. 10)
(x/c)	Chordwise location as a fraction of the local chord
(y/ℓ)	Spanwise location as a fraction of the span
k	Reduced frequency = $\omega c_r/2V$ in subsonic flow
Δp_j	Pressure induced by the downwash of the jth vibration mode
$\bar{L}$, L	Nondimensional lift functions used in Refs. 1 and 2
a_{nm}	Weighting factors in lift distribution
b_{qp}	Weighting factors in downwash distribution
M	Mach number
q	Dynamic pressure
μ	$\ell/b_o \tan\Lambda$

I. INTRODUCTION

In spite of extensive experimental and analytical efforts, the various aerodynamic effects on flutter stability in the transonic regime are not yet well understood. Nor, until recently, has there been much hope of delineating the significance of these effects. With the advent of the NASA Kernel-Function Procedures, progress in this direction now seems possible. Although the procedures are not applicable to the nonlinear transonic regime, they provide nevertheless some of the first insight into wing-loading distribution and unsteady effects at speeds in the neighborhood of Mach 1.

By utilizing the Kernel-Function Procedure at frequencies very close to zero, it is possible to study first-order unsteady effects. By eliminating the $\partial h/\partial x$ contribution to the downwash when the reduced frequency is not zero, it is possible to study quasi-steady effects. In this way, the effect of each characteristic of the aerodynamics can be isolated and studied independently. It will thus become possible to know, for example, the relative importance of the steady-state lift distribution and its subsequent unsteady modifications.

This report is intended to provide a preliminary assessment of the NASA Kernel-Function Procedures and the consequent aerodynamic insight which they provide. The first section of this report illustrates a method of obtaining generalized aerodynamic forces from the results of the Kernel-Function Procedure. The rest of the report compares sample flutter calculations to experimental results, and an attempt is made to explain the discrepancies.

Manuscript released by the authors April 1962 for publication as an ASD Technical Documentary Report.

II. DETERMINATION OF GENERALIZED AERODYNAMIC FORCES

The generalized force, $\hat{Q}_{ij}$, is defined as the "aerodynamic work" done by the jth mode of the wing on the ith mode, i.e.,

$$\hat{Q}_{ij} = \iint_{WING} h_i(\bar{\xi},\bar{\eta})\Delta p_j(\bar{\xi},\bar{\eta})d\bar{\xi}d\bar{\eta} \tag{1}$$

(For definitions of h, $\bar{\xi}$, $\bar{\eta}$, etc., see the LIST OF SYMBOLS.)

A nondimensional generalized force will be defined as follows:

$$Q_{ij} = \frac{1}{C_{L_\alpha}} \iint_{WING} h_i(\bar{\xi},\bar{\eta}) \frac{\Delta p_j(\bar{\xi},\bar{\eta})}{(\rho/2)V^2} \frac{d\bar{\xi}\, d\bar{\eta}}{S} \tag{2}$$

where the normalization is accomplished by dividing by $C_{L_\alpha}(\rho/2)V^2S$ - which is equivalent to the self-induced generalized force for a unit mode shape.

A. RELATIONSHIP TO SUBSONIC KERNEL-FUNCTION LIFT DISTRIBUTION

The subsonic Kernel-Function Procedure (Ref. 1) expresses the pressure in terms of a nondimensional lift function, $\bar{L}(\bar{\xi},\bar{\eta})$, as follows:

$$\frac{\Delta\bar{p}(\bar{\xi},\bar{\eta},t)}{(\rho/2)V^2} = \frac{8\pi\ell}{b_0} L(\bar{\xi},\bar{\eta}) \frac{\bar{q}}{b_0} e^{i\omega t} \tag{3}$$

This pressure amplitude per unit of modeshape j, $\Delta p_j(\xi,\eta)$, is in terms of the pressure, $\Delta\bar{p}(\bar{\xi},\bar{\eta},t)$

$$\Delta p_j(\xi,\eta) = \frac{\Delta\bar{p}(\bar{\xi},\bar{\eta},t)}{(q/b_0)e^{i\omega t}}$$

consequently

$$\frac{\Delta p_j(\bar{\xi},\eta)}{(\rho/2)V^2} = \frac{8\pi\ell}{b_0} \bar{L}_j(\bar{\xi},\bar{\eta}) \tag{4}$$

The root chord of the wing is defined as $2b_0$ and the maximum span as 2ℓ. Nondimensional coordinates are referenced to b_0 and ℓ as follows:

$$\xi = \bar{\xi}/b_0 \qquad \eta = \bar{\eta}/\ell$$

Consequently

$$\frac{d\bar{\xi}\,d\bar{\eta}}{S} = \frac{\ell b_0}{S}\,d\xi\,d\eta \tag{5}$$

Substituting Equations (4) and (5) into (2) yields the generalized force in terms of the lift function and the nondimensional coordinates:

$$Q_{ij} = \frac{2\pi A}{C_{L_\alpha}} \int_{-1}^{1} \int_{\xi_L}^{\xi_T} h_i(\xi,\eta)\ \bar{L}_j(\xi,\eta)\,d\xi\,d\eta \tag{6}$$

where A is the wing aspect ratio, $\frac{(2\ell)^2}{S}$, and ξ_L and ξ_T are the leading- and trailing-edge values of ξ.

B. RELATIONSHIP TO SUPERSONIC KERNEL-FUNCTION LIFT DISTRIBUTION

The supersonic Kernel-Function Procedure (Ref. 2) relates the pressure to a lift function, $L(\bar{\xi},\bar{\eta})$, as follows:

$$\frac{\Delta p_j(\bar{\xi},\bar{\eta})}{(\rho/2)V^2} = 4\pi L_j(\bar{\xi},\bar{\eta}) \tag{7}$$

The root chord is defined as 2b and the maximum span as 4bs. Nondimensional coordinates are defined as

$$\xi = \bar{\xi}/2b \qquad \eta = \bar{\eta}/2b$$

Consequently

$$\frac{d\bar{\xi}\,d\bar{\eta}}{S} = \frac{4b^2}{S}\,d\xi\,d\eta \tag{8}$$

Substituting Equations (7) and (8) into (2) yields for the generalized force:

$$Q_{ij} = \frac{\pi A}{s^2 C_{L_\alpha}} \int_{-s}^{s} \int_{\xi_L}^{\xi_T} h_i(\xi,\eta) L_j(\xi,\eta) d\xi d\eta \qquad (9)$$

C. APPROXIMATE METHOD OF CALCULATING GENERALIZED FORCES

In both the subsonic and supersonic Kernel-Function Procedures the lift function, $L(\xi,\eta)$, is expressed as a polynomial in both coordinates. The procedures determine those coefficients of the assumed polynomial which best satisfy the integral equation for the downwash at a number of "control points" on the wing. In order to evaluate the generalized force it is necessary to (1) determine the lift function, L, by appropriate combination of the coefficients with the terms in the polynomial, (2) multiply the result by the modeshape, h, and (3) integrate the product, both chordwise and spanwise, over the wing. Because some of the significant terms in $L(\xi,\eta)$ are singular at the leading edge, numerical integration is difficult unless special provisions are made. As an alternative it was decided to fit the modeshape, h, by a polynomial in ξ and η and to obtain closed-form integrals for the new L-h product. The details of these calculations are presented below.

1. Subsonic Procedure

The Kernel-Function Procedure utilizes an angular chordwise variable, θ, which is related to ξ as follows:

$$\theta = \cos^{-1} \frac{\xi_T + \xi_L - 2\xi}{\xi_T - \xi_L} \qquad (10)$$

Consequently

$$\sin\theta d\theta = \frac{2d\xi}{\xi_T - \xi_L} = \frac{b_0}{b} d\xi$$

and

$$\xi = \frac{\xi_T + \xi_L}{2} - \frac{\xi_T - \xi_L}{2}\cos\theta$$

The lift function is approximated by an expansion in both the θ and η coordinates:

$$\bar{L}_j(\xi,\eta) = \frac{b_0}{b}\sqrt{1-\eta^2}\left[\sum_m a^j_{nm}\,\eta^m \cot\frac{\theta}{2} + \sum_n\sum_m \frac{4}{2^{2n}}\, a^j_{nm}\,\eta^m \sin n\theta\right] \qquad (11)$$

where the a^j_{nm} are determined as a function of the downwash, w_j, by the Kernel-Function Procedure. Assuming symmetric spanwise modes and multiplying by the differential yields

$$\bar{L}_j(\xi,\eta)d\xi = \sqrt{1-\eta^2}\,\sin\theta\left[\sum\sum a^j_{nm}\, f_n(\theta)\eta^{2m}\right] d\theta \qquad (12)$$

where

$$f_n(\theta) = \cot\frac{\theta}{2},\ \sin\theta,\ \frac{1}{4}\sin 2\theta,\ \frac{1}{16}\sin 3\theta \ \ldots$$

By assuming that $h_i(\xi,\eta)$ can be approximated by the polynomial

$$h_i(\xi,\eta) = \sum_p\sum_q b^i_{qp}\xi^q\eta^{2p} \qquad (13)$$

and substituting Equations (12) and (13) into (6), Q_{ij} becomes a series of basic integrals:

$$Q_{ij} = \frac{4\pi A}{C_{L_\alpha}} \sum_m\sum_n\sum_p\sum_q a^j_{nm}\, b^i_{qp} \int_0^1\int_0^\pi \sqrt{1-\eta^2}\,\sin\theta\, f_n(\theta)\eta^{2(m+p)} \left[\frac{\xi_T + \xi_L}{2} - \frac{\xi_T - \xi_L}{2}\cos\theta\right]^q d\theta d\eta \qquad (14)$$

For a wing with straight leading- and trailing-edges, a midchord sweep angle of Λ, and a taper ratio of $\bar{\lambda}$

$$\frac{\xi_T - \xi_L}{2} = 1 - (1 - \bar{\lambda})\eta \tag{15}$$

$$\frac{\xi_T + \xi_L}{2} = \frac{\ell}{b_o} \tan\Lambda \; \eta = \mu\eta \tag{16}$$

Substituting Equations (15) and (16) into (14) yields an explicit form for Q_{ij}:

$$Q_{ij} = \frac{4\pi A}{C_{L_\alpha}} \sum_m \sum_n \sum_p \sum_q a_{mn}^j \, b_{qp}^i \int_0^1 \int_0^\pi \sqrt{1-\eta^2} \sin\theta \, f_n(\theta) \eta^{2(m+p)}$$

$$\left[\mu\eta - \left\{ 1 - (1-\bar{\lambda})\eta \right\} \cos\theta \right]^q \, d\theta d\eta$$

Expanding $\left[\mu\eta - \left\{ 1-(1-\bar{\lambda})\eta \right\} \cos\theta \right]^q$ twice in binomial series results in the following set of integrals:

$$Q_{ij} = \frac{4\pi A}{C_{L_\alpha}} \sum_m \sum_n \sum_p \sum_q \sum_s \sum_t a_{nm}^j \, b_{qp}^i \, (-)^t \binom{q}{s} \binom{s}{t} \mu^{q-s} \, (1-\bar{\lambda})^{s-t} \, P_{n,\, 2(m+p)+q-t,\, s} \qquad t \le s \le q \tag{17}$$

where

$$P_{n,r,s} = \int_0^1 \int_0^\pi \sqrt{1-\eta^2} \, \eta^r \, f_n(\theta) \cos^s\theta \sin\theta \, d\theta d\eta$$

These integrals are evaluated in Appendix A.

Substituting for the P_{nrs} yields

$$Q_{ij} = \frac{\pi^3 A}{C_{L_\alpha}} \sum_m \sum_n \sum_p \sum_q \sum_s \sum_t a_{nm}^j \, b_{qp}^i \, (-)^t \binom{q}{s} \binom{s}{t} \mu^{q-s} (1-\bar{\lambda})^{s-t}$$

$$\frac{\Gamma\left(\frac{2(m+p)+q+1-t}{2}\right)}{\sqrt{\pi}\,\Gamma\left(\frac{2(m+p)+q+4-t}{2}\right)} \, T(s,n) \tag{18}$$

where $T(s,n)$ is defined in Appendix A.

This expression can be put partly into matrix form as follows:

$$Q_{ij} = \frac{\pi^3 A}{C_{L_\alpha}} \sum_q \sum_p b^i_{qp} \; I^j_{qp} \tag{19}$$

where I^j_{qp} is the sum of the diagonals of the following matrix operation

$$I^j_{qpm} = \left[\frac{(-)^t \, \Gamma\left(\frac{2(m+p)+q+1-t}{2}\right)}{\sqrt{\pi}\,\Gamma\left(\frac{2(m+p)+q+4-t}{2}\right)} \right]_t \left[\binom{s}{t} (1-\bar{\lambda})^{s-t} \right]_s \left[\binom{q}{s} \mu^{q-s} \right]_s \left[T(s,n) \right]_n \left[a^j_{nm} \right]_m \tag{20}$$

and

$$T(s,n) = \begin{matrix} \\ 1 \\ 1/2 \\ 1/2 \\ 3/8 \end{matrix} \begin{matrix} \begin{matrix} n \\ \end{matrix} \\ \begin{bmatrix} 1 & 1/2 & 0 & 0 \\ 1/2 & 0 & 1/16 & 0 \\ 1/2 & 1/8 & 0 & 1/128 \\ 3/8 & 0 & 1/32 & 0 \end{bmatrix} \end{matrix} \begin{matrix} s \\ \\ \\ \\ \\ \end{matrix} \qquad t \le s \le q$$

2. Supersonic Procedure

The lift function is approximated by the following expansion in the ξ and η coordinates:

$$L(\xi,\eta) = \sum \sum a^j_{nm} \; \eta^m \; \ell_n \; (\xi,\eta)$$

where

$$\ell_n \; (\xi,\eta) = \sqrt{\frac{\xi}{(s\xi)^2-\eta^2}}, \sqrt{\frac{\xi^2}{(s\xi)^2-\eta^2}}, \sqrt{(s\xi)^2-\eta^2}, \; \xi\sqrt{(s\xi)^2-\eta^2}, \text{ etc.} \tag{21}$$

Assuming symmetric spanwise modes and replacing $h_i(\xi,\eta)$ by the polynomial $\Sigma\Sigma b^i_{qp}\,\xi^q\eta^{2p}$ yields for Q_{ij}

$$Q_{ij} = \frac{8\pi}{sC_{L_\alpha}} \sum\sum\sum\sum a^j_{nm}\, b^i_{qp} \int_0^1 \int_0^{s\xi} h_p(\xi,\eta)\,\xi^q \eta^{2(m+p)}\, d\eta\, d\xi \qquad (22)$$

$$= \frac{4\pi}{sC_{L_\alpha}} \sum\sum\sum\sum a^j_{nm}\, b^i_{qp}\, K_n(q, m+p)$$

where

$$K_n(=0,1) = \frac{2}{\pi} s^{2(m+p)} \int_0^1 \int_0^1 \xi^{2(m+p)+q+n+1} \frac{\nu^{2(m+p)}}{\sqrt{1-\nu^2}}\, d\nu \quad d\xi$$

$$= \frac{s^{2(m+p)}}{2(m+p)+q+n+2} \frac{\Gamma(m+p+\frac{1}{2})}{\sqrt{\pi}\,\Gamma(m+p+1)}$$

and $K_n(2,3) = \frac{2}{\pi} s^{2(m+p+1)} \int_0^1 \int_0^1 \xi^{2(m+p)+q+n} \nu^{2(m+p)} \sqrt{1-\nu^2}\, d\nu\, d\xi$

$$= \frac{s^{2(m+p+1)}}{2(m+p)+q+n+1} \frac{1}{2(m+p+1)} \frac{\Gamma(m+p+\frac{1}{2})}{\sqrt{\pi}\Gamma(m+p+1)}$$

Consequently

$$Q_{ij} = \frac{4\pi^2}{sC_{L_\alpha}} \sum\sum\sum\sum a^j_{nm}\, b^i_{qp}\, s^{2(m+p)} \frac{\Gamma(m+p+\frac{1}{2})}{\sqrt{\pi}\,\Gamma(m+p+1)}\, f(n, m+p, q) \qquad (23)$$

where $f(n, m+p, q) = \frac{1}{2(m+p)+q+2}, \frac{1}{2(m+p)+q+3}, \frac{s^2}{2(2(m+p)+q+3)(m+p+1)},$

$$\frac{s^2}{2(2(m+p)+q+4)(m+p+1)}$$

Writing partly in matrix form yields

$$Q_{ij} = \frac{4\pi^2}{sC_{L_\alpha}} \sum\sum b^i_{qp} \; r^j_{qp} \tag{24}$$

where r^j_{qp} is the sum of the diagonals of the matrix operation

$$r^j_{qpm} = \left[s^{2(m+p)} \frac{\Gamma(m+p+1/2)}{\sqrt{\pi}\,\Gamma(m+p+1)} \right] x$$

$$\left[\frac{1}{2(m+p)+q+2} \quad \frac{1}{2(m+p)+q+3} \quad \frac{1}{2(2(m+p)+q+3)(m+p+1)} \quad \frac{s^2}{2(2(m+p)+q+4)(m+p+1)} \right] x$$

$$\left[a^j_{nm} \right] \tag{25}$$

In order to evaluate Q_{ij} in Equations (19) and (24) it is necessary to obtain a^j_{nm}, the coefficients of the lift-distribution polynomial, as a function of the wing-downwash distribution. The wing-downwash distribution is given as

$$\frac{w_j(x,y)}{V} = \frac{\partial h_j}{\partial x}(x,y) + ikh_j(x,y) \tag{26}$$

where k is the reduced frequency. Calculating the downwash according to Equation (26) and substituting into the Kernel-Function Program yields the a^j_{nm}. The corresponding Q_{ij} are defined as:

$$Q_{ij} = Q_{\Theta_{ij}}(k) = Q_{\alpha_{ij}}(k) + ik\,Q_{h_{ij}}(k) \tag{27}$$

Expanding in powers of k yields

$$Q_{ij} = Q_{\theta_{ij}} + ik\, Q_{\dot{\theta}_{ij}} + \frac{(ik)^2}{2!} Q_{\ddot{\theta}_{ij}} + \cdots \tag{28}$$

where

$$Q_{\theta_{ij}} = Q_{\alpha_{ij}}$$

$$Q_{\dot{\theta}_{ij}} = Q_{\dot{\alpha}_{ij}} + Q_{h_{ij}}$$

$$Q_{\ddot{\theta}_{ij}} = Q_{\ddot{\alpha}_{ij}} + Q_{\dot{h}_{ij}} \quad \text{etc.}$$

In order to evaluate the various generalized force contributions, it is necessary only to substitute the appropriate downwash contribution of Equation (26) into the Kernel-Function Program and to utilize Equation (19) or (24). The location and number of control points used for the evaluation of a^j_{nm} and b^i_{qp} will be discussed in the following section.

III. EVALUATION OF FLUTTER CHARACTERISTICS FOR A UNIFORM 70° DELTA WING

In this section a cantilevered 70° delta wing made of aluminum, having a root chord of 4 ft and a constant thickness of .128 in., will be analyzed. The vibration modes are given in Table 1. These modes were taken from Ref. 3, in which the wing has a root chord of 1 ft and a thickness of .032 in. Consequently, while the modes are similar, the frequencies of Ref. 3 are four times those encountered here.

A. APPROXIMATION OF VIBRATION MODES

Before any evaluation of the generalized force can be made, the downwash distribution must be computed for each mode. If the wing is presumed to oscillate at a frequency, ω, the relation for the downwash is

$$\frac{w_j}{V} = \frac{\partial h_j}{\partial x} + ikh_j$$

where k is the reduced frequency $\omega c_r/2V$ and $\omega c_r/V$ in subsonic and supersonic flow, respectively.

The generalized force resulting from $\partial h_j/\partial x$ is defined as $Q_{\alpha_{ij}}$, whereas the term resulting from h_j is defined as $Q_{h_{ij}}$. The h_j component of the downwash is directly obtainable from the modeshape data in Table 1. The $\partial h_j/\partial x$ component is obtained by numerically differentiating the data in Table 1 with respect to the nondimensional chordwise coordinate. The result is presented in Table 2 for the same chordwise and spanwise locations. Each table gives 46 values of downwash contribution; the Kernel-Function Programs, however, allow for only about 16 downwash values or "control points." Since the major generalized force contributions normally come from the outboard portions of the wing (inboard contributions are doubly small because both the lift and modeshape values are small), downwash values will be utilized for the 16 points corresponding to $(x/c) = .25, .50, .75, 1.00$; $(y/\ell) = .3, .5, .7, .9$. The coordinates (x/c) and (y/ℓ) represent percentages of the local chord and semispan respectively. The former corresponds to $\bar{x}$ in NASA's subsonic Kernel-Function Program.

The modeshapes and derivatives in Tables 1 and 2 can be utilized directly in NASA's supersonic program. For the subsonic program, however, the derivative

$$(\partial h/\partial \bar{x})_{\text{Ref. 1}} = 2\left[1-(y/\ell)\right]\partial h/\partial x \qquad (29)$$

is used as an input.

The input coordinates in supersonic flow are referenced to the wing apex as follows:

$$y = s(y/\ell) \tag{30}$$

and

$$x = \left[1-(y/\ell)\right]\ (x/c) + (y/\ell) \tag{31}$$

In subsonic flow, the coordinates (x/c) and (y/ℓ) are used directly.

After the corresponding a^j_{nm} terms have been evaluated it is necessary to approximate the modeshape $h_i\ (\xi,\eta)$ by a least-squares polynomial before Equations (19) and (24) can be used. Specifically, this involves finding a surface, $h_i = \sum_p \sum_q b^i_{qp}\, \xi^q \eta^{2p}$, for which the sum of the squared differences between the modeshape values and the surface are a minimum. The coordinates ξ and η are defined in terms of (x/c) and (y/ℓ) as follows:

1. Subsonic Flow

$$\xi = 2\left[1-(y/\ell)\right]\ (x/c) + 2(y/\ell)-1;\ \eta = (y/\ell)$$

2. Supersonic Flow

$$\xi = \left[1-(y/\ell)\right]\ (x/c) + (y/\ell);\ \eta = s(y/\ell)$$

Assuming both q and p range from 0 to 3, the least-squares solution for b^i_{qp} is

$$\left\{b^i_{qp}\right\}_{q,p} = \left(\left[\sum_{s,r} F(s+q,\ r+p)\right]\right)^{-1}_{s,r} \left\{G_i(s,r)\right\}$$

where

$$\left[G_i(s,r)\right]_{s}^{r} = \left[\xi_t^{\,s}\right]_{s}^{t} \left|h_i(\xi_t,\eta_t)\right| \left[\eta_t^{\,2r}\right]_{t}^{r}$$

and

$$\left[F(s+q, r+p)\right]^{s+q \backslash r+p} = \left[\xi_t^{s+q}\right]^{s+q \backslash t} \left[\eta_t^{2(r+p)}\right]^{t \backslash r+p}$$

The subscript, t, refers to the 46 coordinate locations and mode-shape values given in Table 1. The above operations involve considerable reorganization of matrix elements; consequently the procedure has been programed on the IBM 7090. The b^i_{qp} corresponding to the subsonic coordinates are presented in Table 3 for the first three vibration modes of the wing. The corresponding supersonic b^i_{qp} can be obtained from the subsonic matrix by using pre- and post-multiplying transformation matrices as follows:

$$\left[b^i_{qp_{super.}}\right] = \begin{bmatrix} 1 & -1 & 1 & 1 \\ 0 & 2 & -4 & 6 \\ 0 & 0 & 4 & -12 \\ 0 & 0 & 0 & 8 \end{bmatrix} \left[b^i_{qp_{sub.}}\right] \begin{bmatrix} 1 & & & \\ & 1/s^2 & & \\ & & 1/s^4 & \\ & & & 1/s^6 \end{bmatrix}$$

B. EVALUATION OF GENERALIZED FORCES

The downwash corresponding to the modes in Table 1 has been inserted into both the subsonic and supersonic Kernel-Function Procedures. In the former case, all results satisfy the necessary reversibility conditions to within 10% (e.g., the generalized forces, $Q_{h_{ij}}$, in forward flow are equal to those in reverse flow, with the modes interchanged). Moreover, the stability derivatives for translating and pitching modes agree well with those of other formulations. The supersonic Kernel Function, however, did not meet with such success. In fact it was not even possible to obtain a reasonable value of C_{L_α} with the control points selected. By choosing control-point locations primarily on the inboard portion of the wing, an accurate estimate of C_{L_α} can be obtained; however, this selection of control points fails completely to

reflect the rapid downwash variations on the outer portion of the wing. This conclusion was confirmed by a letter to Aerojet-General from NASA, who agreed that the supersonic Kernel Function was not yet in a form to handle the mode-shapes analyzed here. Accordingly, all remaining calculations will be performed for subsonic speeds only.

1. Quasi-Steady Analysis

In order to assess the importance of transients, generalized forces and flutter conditions will be computed for quasi-steady, first-order unsteady, and general unsteady flow conditions.

For quasi-steady flow, the real part of the generalized force is obtained from the a^j_{nm} corresponding to the downwash, $\partial h_j/\partial x$, when the reduced frequency parameter, k, is zero. The imaginary part of the generalized force is obtained from the a^j_{nm} corresponding to the downwash, kh_j, divided by the reduced frequency k, in the limit as k approaches zero. All of the a^j_{nm} are given in Appendix B for Mach number 0. The resulting generalized force matrices are defined as $Q_{\alpha_{ij}}$ and $Q_{h_{ij}}$ respectively. The former corresponds to steady-state effects, the latter to quasi-steady effects.

In flutter analyses, whenever the generalized forces are encountered they are divided by corresponding generalized masses. Accordingly, from now on the ratio of the generalized forces to generalized masses will be given. For the wing analyzed here, the mass density is a constant and the generalized masses (normalized by the total wing mass) are nothing more than the h_i-h_j products integrated over the wing. The results of the double numerical integration for the three modes of Table 1 are given below:

$$\left[\bar{m}\right] = \left[h_i\right]\left[m/m_o\right]\left[h_j\right] = \begin{bmatrix} .0741 & .0000 & .0103 \\ .0000 & .1430 & -.0321 \\ .0103 & -.0321 & .2115 \end{bmatrix} \qquad (32)$$

If the modes are to be orthogonal, the off-diagonal elements should be zero. It is apparent, however, when the third mode is involved, that the numerical integration of the modeshape products over the 46 control points is somewhat inaccurate. Furthermore if 46 control points are insufficient to accurately evaluate the generalized masses they will be even less sufficient to evaluate the generalized aerodynamic forces. In spite of the inaccuracies, calculations will be made, henceforth, for all three modes; third mode effects, however, will be regarded as qualitative in nature.

The ratios of generalized forces to masses are defined as follows:

$$\left[\bar{Q}_{ij}\right] = \left[\bar{m}\right]^{-1}\left[Q_{ij}\right] \tag{33}$$

Off-diagonal elements of the $\bar{m}$ matrix will be ignored in all calculations.

These matrices have been computed by using the NASA Kernel-Function Procedure and Equations (19) and (24). Both the real and imaginary parts, $\bar{Q}_{\alpha_{ij}}$ and $\bar{Q}_{h_{ij}}$, are presented in Appendix C for Mach numbers 0, .5, .7, .8, and .9.

2. First-Order Unsteady Analysis

Here, in addition to the quasi-steady terms, the first-order unsteady term, $\bar{Q}_{\dot{\alpha}_{ij}}$, is also included. While no change results in the real part of the $\bar{Q}_{ij}$ matrix, the imaginary part is now the sum of the quasi-steady and first-order unsteady terms - that is, $\bar{Q}_{\theta_{ij}} = \bar{Q}_{h_{ij}} + \bar{Q}_{\dot{\alpha}_{ij}}$. Consequently the necessary a^j_{nm} are obtained for the downwash $\partial h_j/\partial x + ikh_j$ in the limit as k approaches zero.

3. General Unsteady Flow Analysis

Here the reduced frequency of interest is substituted directly into the NASA Kernel-Function Procedure. Both the real and the imaginary

part of the generalized force correspond to the downwash $\partial h_j/\partial x + ikh_j$. The imaginary part, however, is divided by the reduced frequency as before. Consequently these values will reduce to the first-order unsteady ones as k approaches zero.

C. EVALUATION OF FLUTTER CONDITIONS

In performing the flutter analysis, only the first two wing vibration modes will be considered. The accuracy of higher-order modeshape calculations is dubious; furthermore their effect is of second order for the type of wing analyzed here. In addition, the effect of structural damping is ignored.

The flutter determinant yields the following two equations (this result will be derived in an ASD report to be published early in 1962):

$$\left(\frac{\omega_f}{\omega_2}\right)^2 = \frac{1}{2}\left[\left(\frac{\omega_1^2}{\omega_2^2} + \lambda\,\bar{Q}_{R_{11}}\right) + \left(1+\lambda\,\bar{Q}_{R_{22}}\right) \pm \sqrt{\left[\left(\frac{\omega_1^2}{\omega_2^2} + \lambda\,\bar{Q}_{R_{11}}\right) - \left(1+\lambda\bar{Q}_{R_{22}}\right)\right]^2 + 4\lambda^2\bar{Q}_{R_{12}}\,\bar{Q}_{R_{21}}}\right] \tag{34}$$

$$\left(\frac{\omega_f}{\omega_2}\right)^2 = \frac{1}{\bar{Q}_{I_{11}} + \bar{Q}_{I_{22}}}\left[\bar{Q}_{I_{22}}\left(\frac{\omega_1^2}{\omega_2^2} + \lambda\bar{Q}_{R_{11}}\right) + \bar{Q}_{I_{11}}\left(1 + \lambda\bar{Q}_{R_{22}}\right) - \lambda\left(\bar{Q}_{R_{12}}\,\bar{Q}_{I_{21}} + \bar{Q}_{R_{21}}\,\bar{Q}_{I_{12}}\right)\right] \tag{35}$$

where ω_1, ω_2 and ω_f are the vibration and flutter frequencies, $\bar{Q}_{R_{ij}}$ and $\bar{Q}_{I_{ij}}$ are the real and imaginary parts of the generalized force-mass ratios, and λ is a flutter dynamic-pressure parameter defined as

$$\lambda = \frac{q_f S C_{L_\alpha}}{m_0 c_r \omega_2^2}$$

where q_f is the dynamic pressure at flutter, S is the wing area, m_0 its mass, and c_r its root chord.

The following values will be used in the calculation

$\omega_1 = 18.7$ cps

$\omega_2 = 43.2$ cps

$S = 2.9$ sq ft

$c_r = 4$ ft

$m_0 = .161$ slugs

Except for a factor of 4 in the model size and frequencies, these correspond to the values encountered in Ref. 3.

The simultaneous solution of Equations (34) and (35) for λ is given on page 18, followed by the corresponding solution for the frequency.

$$\lambda = \frac{\left(1 - \frac{\omega_1^2}{\omega_2^2}\right)}{\left(\bar{Q}_{I_{11}} + \bar{Q}_{I_{22}}\right)\sqrt{-\frac{\bar{Q}_{R_{12}}\bar{Q}_{R_{21}}}{\bar{Q}_{I_{11}}\bar{Q}_{I_{22}}} + \left(\frac{\bar{Q}_{I_{12}}\bar{Q}_{R_{21}} + \bar{Q}_{I_{21}}\bar{Q}_{R_{12}}}{2\bar{Q}_{I_{11}}\bar{Q}_{I_{22}}}\right)^2} + \left(\bar{Q}_{R_{11}} - \bar{Q}_{R_{22}}\right) - \frac{\left(\bar{Q}_{I_{11}} - \bar{Q}_{I_{22}}\right)\left(\bar{Q}_{I_{22}}\bar{Q}_{R_{21}} + \bar{Q}_{I_{21}}\bar{Q}_{R_{12}}\right)}{2\bar{Q}_{I_{11}}\bar{Q}_{I_{22}}}} \tag{36}$$

18

$$\left(\frac{\omega_f}{\omega_2}\right)^2 = \frac{\left(\bar{Q}_{I_{11}} + \frac{\omega_1^2}{\omega_2^2}\bar{Q}_{I_{22}}\right)\sqrt{-\frac{\bar{Q}_{R_{12}}\bar{Q}_{R_{21}}}{\bar{Q}_{I_{11}}\bar{Q}_{I_{22}}} + \left(\frac{\bar{Q}_{I_{12}}\bar{Q}_{R_{21}} + Q_{I_{21}}\bar{Q}_{R_{12}}}{2\bar{Q}_{I_{11}}\bar{Q}_{I_{22}}}\right)^2} + \left(Q_{R_{11}} - \frac{\omega_1^2}{\omega_2^2}\bar{Q}_{R_{22}}\right) - \frac{\left(\bar{Q}_{I_{11}} - \frac{\omega_1^2}{\omega_2^2}\bar{Q}_{I_{22}}\right)\left(\bar{Q}_{I_{12}}\bar{Q}_{R_{21}} + \bar{Q}_{I_{21}}\bar{Q}_{R_{12}}\right)}{2\bar{Q}_{I_{11}}\bar{Q}_{I_{22}}}}{\left(\bar{Q}_{I_{11}} + \bar{Q}_{I_{22}}\right)\sqrt{-\frac{\bar{Q}_{R_{12}}\bar{Q}_{R_{21}}}{\bar{Q}_{I_{11}}\bar{Q}_{I_{22}}} + \left(\frac{\bar{Q}_{I_{12}}\bar{Q}_{R_{21}} + \bar{Q}_{I_{21}}\bar{Q}_{R_{12}}}{2\bar{Q}_{I_{11}}\bar{Q}_{I_{22}}}\right)^2} + \left(\bar{Q}_{R_{11}} - \bar{Q}_{R_{22}}\right) - \frac{\left(\bar{Q}_{I_{11}} - \bar{Q}_{I_{22}}\right)\left(\bar{Q}_{I_{22}}\bar{Q}_{R_{21}} + \bar{Q}_{I_{21}}\bar{Q}_{R_{12}}\right)}{2\bar{Q}_{I_{11}}\bar{Q}_{I_{22}}}} \tag{37}$$

1. Quasi-Steady Analysis

For quasi-steady flow $\bar{Q}_{R_{ij}} \longrightarrow \bar{Q}_{\alpha_{ij}}$ and $\bar{Q}_{I_{ij}} \longrightarrow k\,\bar{Q}_{h_{ij}}$.

Consequently, the real and imaginary part of the $\bar{Q}_{ij}$ matrix in Equations (36) and (37) can be replaced by $\bar{Q}_{\alpha_{ij}}$ and $\bar{Q}_{h_{ij}}$ respectively. These values are given in Appendix III. When substituted into Equations (36) and (37), the following flutter dynamic pressures and frequencies are obtained for various Mach numbers:

	Mach Number				
	0	0.5	0.7	0.8	0.9
Dynamic pressure (psi)	560	550	545	545	570
Frequency (cps)	238	238	237	235	232

The dynamic pressures and frequencies are plotted as a function of Mach number in Figures 2 and 3 respectively. Results are compared with the experimental data of Ref. 3. Also shown in the figures are theoretical values obtained from piston theory, modified piston theory (adjusted for the correct C_{L_α}), the first-order unsteady Kernel Function, and the general unsteady Kernel Function.

2. First-Order Unsteady Analysis

As in the quasi-steady analysis $\bar{Q}_{R_{ij}} \longrightarrow \bar{Q}_{\alpha_{ij}}$; however, $\bar{Q}_{I_{ij}}/k$ now becomes $\bar{Q}_{\dot{\theta}_{ij}} = \bar{Q}_{h_{ij}} + \bar{Q}_{\dot{\alpha}_{ij}}$. The first order term in k now includes, in addition to the quasi-steady term due to h, an unsteady term due to $\frac{\partial h}{\partial x}$. The latter effects are similar to those of $C_{L_{\dot{\alpha}}}$ and $C_{M_{\dot{\alpha}}}$ in two-degrees-of freedom flutter.

Values of $\bar{Q}_{\dot{\theta}_{ij}}$ are also given in Appendix C ; when substituted together with $\bar{Q}_{\alpha_{ij}}$ into Equations (36) and (37), the following results are obtained at flutter.

	Mach Number				
	0	0.5	0.7	0.8	0.9
Dynamic pressure (psi)	565	645	705	740	755
Frequency (cps)	238	228	219	212	199

These results are also presented in Figures 2 and 3.

3. General Unsteady Analysis

Here, the real and imaginary $\bar{Q}_{ij}$, $\bar{Q}_{R_{ij}}$ and $\bar{Q}_{I_{ij}}$, which are given in Appendix C for the reduced frequency (k = .6), can easily be substituted directly into Equations (36) and (37). These results are presented below for k = .5, .6, and .75.

	Mach Number				
Reduced Frequency, k = .5	0	0.5	0.7	0.8	0.9
Dynamic pressure (psi)	530	615	685	710	735
Frequency (cps)	241	232	221	212	198
Reduced Frequency, k = .6					
Dynamic pressure (psi)	515	610	675	705	720
Frequency (cps)	241	232	222	212	198
Reduced Frequency, k = .75					
Dynamic pressure (psi)	530	600	660	690	690
Frequency (cps)	242	232	221	207	194

These results are used to calculate the flutter conditions for the flutter reduced frequency; these are also shown in Figures 2 and 3. It is apparent from the figures that unsteady effects above the first order have only a minor influence on the flutter conditions. There is a significant difference, however, especially at the higher Mach numbers, between the first-order unsteady results and the quasi-steady results. Most of this difference

is a direct result of the radical differences in the 2,2 elements of the generalized-force matrices. For the first-order unsteady case, $\bar{Q}_{\dot{\theta}_{22}}$ becomes very large with a change in Mach number, whereas $\bar{Q}_{h_{22}}$ varies only slightly. The effect of the large $\bar{Q}_{\dot{\theta}_{22}}$ is to increase the flutter speed. The experimental data, however, indicate that the quasi-steady flutter-speed predictions are much superior to those of unsteady flow. It appears that the large transient effects predicted by linearized theory in the transonic regime are not actually realized. Comparisons with the experimental frequencies further support this thesis.

It should be remarked that the piston-theory predictions shown in Figures 2 and 3 produce only an apparent agreement with the data for subsonic Mach numbers. For this particular wing, radically incorrect values of the lift-curve slope and aerodynamic center compensate in such a way as to approximate the actual flutter speed and frequency. When the proper C_{L_α} is used (this would be required for the simple modes of a pitch-roll coupling analysis) highly erroneous flutter conditions are predicted.

IV. CONCLUSIONS

A method has been described for utilizing the NASA Kernel-Function Procedures to determine generalized aerodynamic forces and the subsequent flutter conditions. The subsonic procedure was found to work quite well; all results satisfy the necessary reversibility conditions to within 10%; in addition the stability derivatives for translating and pitching modes agree with those of other formulations. The supersonic procedure did not meet with such success. For the wing and modeshapes encountered in this report, it was not even possible to obtain a reasonable value of C_{L_α} with the control points selected. By choosing control-point locations primarily on the inboard portion of the wing, an accurate estimate of C_{L_α} could be obtained; however, this selection of control points cannot reflect the rapid downwash variations on the outer portion of the wing. This conclusion was confirmed in a latter from NASA to Aerojet-General, which stated that the supersonic Kernel Function was not yet in a form to handle the modeshapes encountered here.

A flutter analysis was performed on a uniform, cantilevered, 70° delta wing using the NASA subsonic Kernel-Function Procedure. Three sets of analyses were performed for a range of subsonic Mach numbers. These included a quasi-steady analysis (all transients neglected), a first-order unsteady analysis (includes transients up to the order of k), and a complete unsteady analysis corresponding to the reduced frequency at flutter. The following conclusions were reached:

1. The first order approximation, which assumes that a power-series expansion of the unsteady effects is valid, yields, for this wing, flutter conditions in the high subsonic range which are very close to those of the complete unsteady analysis.

2. The quasi-steady analysis differs significantly from the first-order or general unsteady analysis at the higher subsonic Mach numbers. The primary reason arises from the large $\dot{\alpha}$ effects which are predicted by linearized theory. The damping normally resulting from these $\dot{\alpha}$ effects is not present in a quasi-steady analysis, and thus the latter will lead to lower flutter-speed predictions.

3. For the 70° delta wing analyzed in this report, the quasi-steady analysis gives the best correlation with experimental flutter results. Apparently the actual transients may not be so large as those predicted by linear theory. Consequently, the use of an indicial function or power-series representation of the aerodynamics seems quite reasonable for this type of wing planform. Furthermore analytical or, better, experimental steady and quasi-steady aerodynamics seem to provide a significant portion of the actual aerodynamic effects on flutter stability.

REFERENCES

1. D. S. Woolston, J. Cunningham, and E. Watkins, An IBM-704 Program of a Kernel-Function Procedure for Obtaining Aerodynamic Forces on Finite Wings in Subsonic Flow, NASA Memorandum for Files, April 1959.

2. H. J. Cunningham, C. E. Watkins, and D. E. Woolston, A Systematic Kernel-Function Procedure for Determining Aerodynamic Forces on Oscillating or Steady Finite Wings With Subsonic Leading Edges and Supersonic Trailing Edges, and a Description of Coding the Procedure for an IBM-704 Computing Machine, NASA Memorandum for Files, December 1959.

3. Perry W. Hanson and Gilbert M. Levy, Experimental and Calculated Results of a Flutter Investigation of Some Very-Low-Aspect-Ratio Flat-Plate Surfaces at Mach Numbers from 0.62 to 3.00, NASA TM X-53, August 1959

APPENDIX A

EVALUATION OF THE INTEGRALS P_{nrs}

The following set of integrals was encountered in the formulation of the generalized force:

$$P_{nrs} = \int_0^1 \int_0^\pi \sqrt{1-\eta^2}\, \eta^r f_n(\theta) \cos^s\theta \sin\theta \, d\theta \, d\eta$$

when

$$n = 0 \quad f_n(\theta) \equiv \cot\frac{\theta}{2} \text{ and}$$

$$P_{ors} = \int_0^1 \int_0^\pi \sqrt{1-\eta^2}\, \eta^r \cos^s\theta \,(1+\cos\theta)\, d\theta \, d\eta$$

Consequently

$$P_{ors} = \begin{cases} \dfrac{\pi^2}{4} \dfrac{\Gamma(r/2+1/2)}{\sqrt{\pi}\,\Gamma(r/2+2)} \dfrac{\Gamma(s/2+1/2)}{\sqrt{\pi}\,\Gamma(s/2+1)} & \text{when s is even} \\ \dfrac{\pi^2}{4} \dfrac{\Gamma(r/2+1/2)}{\sqrt{\pi}\,\Gamma(r/2+2)} \dfrac{\Gamma(s/2+1)}{\sqrt{\pi}\,\Gamma(s/2+1+1)} & \text{when s is odd} \end{cases}$$

For $n \geq 1$, $f_n(\theta) = \dfrac{4}{2^{2n}} \sin n\theta = \dfrac{4}{2^{2n}} \dfrac{\cos(n-1)\theta - \cos(n+1)\theta}{2\sin\theta}$

$$P_{nrs} = \frac{4}{2^{2n+1}} \int_0^1 \int_0^\pi \sqrt{1-\eta^2}\, \eta^r \left\{\cos(n-1)\theta - \cos(n+1)\theta\right\} d\theta d\eta$$

$\cos^s\theta$ can be expanded in series as follows:

$$\cos^s\theta = \frac{1}{2^{(s-1)}} \left(\cos s\theta + s\cos(s-2)\theta + \binom{s}{2} \cos(s-4)\theta \ldots.\right)$$

Consequently, P_{nrs} is zero except when n = s+1, s-1, s-3, etc.

When n = s+1, $P_{nrs} = \frac{\pi^2}{2^{2n+s+1}} \frac{\Gamma(r/2+1/2)}{\sqrt{\pi}\ \Gamma(r/2+2)}$.

When n = s-1, $P_{nrs} = \frac{n\pi^2}{2^{2n+s+1}} \frac{\Gamma(r/2+1/2)}{\sqrt{\pi}\ \Gamma(r/2+2)}$.

When n = s-3, $P_{nrs} = \frac{ns\pi^2}{2^{2n+s+2}} \frac{\Gamma(\ /2+1/2)}{\sqrt{\pi}\ \Gamma(r/2+2)}$.

For a given r the matrix for P_{nrs} can be written as follows:

$$P_{nrs} = \frac{\pi^2}{4} \frac{\Gamma\left(\frac{r+1}{2}\right)}{\Gamma(r/2+2)} T(s,n)$$

s \ n			
1	1/2	0	0
1/2	0	1/16	0
1/2	1/8	0	1/128
3/8	0	1/32	0

APPENDIX B

VALUES OF LIFT DISTRIBUTION WEIGHTING FACTORS FOR SUBSONIC FLOW (M = 0)

Quasi-Steady Case ($k \longrightarrow 0$)

Real part of a^j_{nm} ($w = \partial h_j/\partial x$, $k = 0$):

$M = 0$ ($C_L = 1.794$)

a_{nm} mode 1

.00123	.02706	.22806	.20683
-.01962	-.05382	.43254	-.40048
.02986	-.96989	2.80800	-1.95752
.20071	-1.36891	3.01800	-1.94458

a_{nm} mode 2

.00960	0.06602	-.18883	.15710
-.12993	-.36206	1.39147	-.95197
.11640	1.44379	-6.40412	5.15996
.57116	-5.35124	22.15495	-20.38743

a_{nm} mode 3

.19687	-.92707	1.08853	-.11232
-.21401	2.87112	-4.63879	1.64469
-1.71909	-3.74036	28.52781	-24.58241
.39440	-10.25557	19.38552	-7.51705

Imaginary Part of a^j_{nm}:

a_{nm} mode 1

-.00070	.00417	-.01252	.00696
-.00027	-.01250	.02727	-.01449
.00741	-.03437	.04706	-.01639
.00912	-.02131	-.01069	.03042

a_{nm} mode 2

-.00145	.02237	-.05578	.03622
.00107	-.04792	.11339	-.07313
.02753	-.08816	.20063	-.16219
.00646	-.24977	.91857	-.75926

a_{nm} mode 3

-.00303	.00100	-.00139	.00415
.00074	-.00453	-.00259	-.00032
.01849	-.01815	-.00298	.05440
-.14939	.10584	.00908	-.10722

First Order Unsteady Case ($k \rightarrow 0$)

Real part of a^j_{nm} (same as quasi-steady case).

Imaginary part of a^j_{nm}:

a_{nm} mode 1

-.00077	.00493	-.01366	.00767
-.00066	-.01764	.03983	-.02178
.01094	-.04911	.06394	-.02128
.01045	-.00906	-.06692	.07707

a_{nm} mode 2

-.00118	.02790	.07282	.05166
-.00075	-.07292	.17877	-.11530
.04543	-.11984	.24948	-.21028
-.00530	-.36459	1.44564	-1.21736

a_{nm} mode 3

-.00628	.05924	-.15383	.10329
.01281	-.13010	.36949	-.26883
.03029	-.73351	1.70590	-1.00830
.30396	-.80068	-.34388	1.08629

General Unsteady Case (k= .6)

A value of $k = .6$ is selected merely as a representative case. The actual flutter reduced frequency varies considerably with Mach number.

Real part of a^j_{nm}:

a_{nm} mode 1

.00125	.02488	-.22411	.20440
-.01834	-.04363	.41669	-.39673
.02356	-.97393	2.84633	-1.98638
.20788	-1.37260	3.00610	-1.93194

a_{nm} mode 2

.00893	-.06022	-.18595	.15191
-.12981	-.37300	1.42785	-.97967
.11874	1.38198	-6.29658	5.11130
.62966	-5.48626	22.21595	-20.36997

a_{nm} mode 3

.19733	-.96379	1.13792	-.13451
-.23746	2.97496	-4.78319	1.70721
-1.77164	-3.57096	28.49689	-24.68612
.29564	-10.25408	20.01111	-8.08395

Imaginary part of a_{nm}^{j}:

a_{nm} mode 1

-.00457	.02956	-.08170	.04592
-.00388	-.10570	.23865	-.13059
.06555	-.29394	.38238	-.12736
.06258	-.05232	-.40519	.46386

a_{nm} mode 2

-.00776	.16509	-.43418	.30754
-.00557	-.43537	1.06742	-.68676
.27290	-.71751	1.48607	-1.24835
-.03057	-2.18586	8.65321	-7.28041

a_{nm} mode 3

-.03421	.36086	-.92863	.62460
.08004	-.78606	2.22856	-1.62540
.18012	-4.39795	10.25147	-6.08066
1.81631	-4.78034	-2.05758	6.47860

APPENDIX C

RATIOS OF GENERALIZED AERODYNAMIC FORCES TO MASSES ($\bar{Q}_{ij}$)

I. QUASI-STEADY CASE

A. Real Part of $\bar{Q}_{ij} = (\bar{Q}_{\alpha_{ij}})$:

M = 0 (C_{L_α} = 1.794)			M = .5 (C_{L_α} = 1.848)			M = .7 (C_{L_α} = 1.912)		
.73	7.50	-11.10	.73	7.62	-11.46	.74	7.78	-11.93
-.64	-3.21	2.58	-.64	-3.19	2.44	-.65	-3.16	2.26
.07	1.37	-3.83	.08	1.42	-3.97	.09	1.47	-4.14

M = .8 (C_{L_α} = 1.964)			M = .9 (C_{L_α} = 2.043)		
.74	7.90	-12.35	.73	8.08	-13.07
-.66	-3.13	2.11	-.67	-3.07	1.82
.10	1.52	-4.28	.12	1.59	-4.47

B. Imaginary Part of $\bar{Q}_{ij}/k = (\bar{Q}_{h_{ij}})$:

M = 0			M = .5			M = .7		
1.31	1.77	2.76	1.33	1.85	3.57	1.36	1.96	4.96
-.40	.55	.12	-.39	.58	-.29	-.38	.63	-1.05
.17	.34	-1.03	.17	.35	-1.15	.18	.35	-1.35

M = .8			M = .9		
1.39	2.06	6.57	1.44	2.26	10.24
-.37	.67	-1.91	-.34	.75	-3.58
.19	.35	-1.56	.20	.34	-1.98

II. FIRST-ORDER UNSTEADY CASE

A. Real Part of $\bar{Q}_{ij}$:

This is the same as for the quasi-steady case.

B. Imaginary Part of $\bar{Q}_{ij}/k = (\bar{Q}_{\Theta_{ij}})$:

M = 0			M = .5			M = .7	
1.52	2.59	-1.31	1.55	2.60	-1.07	1.59	2.61	-.73
-.51	.74	-2.67	-.48	1.00	-3.27	-.44	1.39	-4.15
.21	.58	.43	.23	.61	.55	.27	.65	.80

M = .8			M = .9		
1.63	2.63	-.44	1.71	2.72	.03
-.40	1.76	-5.04	-.32	2.53	-6.87
.30	.65	1.12	.36	.58	1.95

III. GENERAL UNSTEADY CASE (k= .6)

A. Real Part of $\bar{Q}_{ij}$:

M = 0			M = .5			M = .7	
.65	7.34	-10.48	.66	7.50	-10.86	.68	7.72	-11.40
-.63	-3.23	2.17	-.65	-3.25	2.03	-.69	-3.27	1.81
.06	1.36	-3.99	.07	1.41	-4.17	.08	1.51	-4.45

M = .8			M = .9		
.69	7.93	-11.93	.73	8.34	-12.90
-.73	-3.28	1.54	-.80	-3.10	.47
.90	1.63	-4.76	.16	1.96	-5.39

B. Imaginary Part of $\bar{Q}_{ij/k}$:

M = 0			M = .5			M = .7		
1.50	2.81	-2.05	1.54	2.84	-1.88	1.59	2.88	-1.59
-.50	.63	-2.24	-.47	.89	-2.81	-.43	1.29	-3.71
.21	.57	.47	.24	.61	.60	.28	.66	.87

M = .8			M = .9		
1.63	2.90	-1.28	1.72	2.84	-.33
-.39	1.73	-4.67	-.24	2.73	-6.68
.32	.66	1.27	.41	.34	3.03

TABLE 1

MODESHAPES FOR CANTILEVERED DELTA WING

Normalized Values of h at y/ℓ =

x/c	0.10	0.20	0.30	0.40	0.50	0.60	0.70	0.80	0.90	1.00
					h_1					
0	0.004	0.012	0.019	0.033	0.060	0.130	0.331	0.550	0.775	
.25	.009	.018	.033	.062	.124	.275	.443	.625	.810	
.50	.014	.034	.061	120	.233	.363	.514	.670	.830	1.000
.75	.023	.082	.152	235	.353	.465	.587	.715	.850	
1.00	.058	.131	.216	306	.418	.525	.639	.750	.875	
					h_2					
.0	-0.019	-0.045	-0.11	-0.345	-0.719	-0.900	-0.836	-0.415	0.190	
.25	-.042	-.135	-.348	-.600	-.741	-.800	-.676	-.255	.330	
.50	-.100	-.225	-.44	-.560	-.555	-.600	-.353	.100	.550	1.000
.75	-.023	-.060	-.124	-.160	0.084	.115	.321	.550	.770	
1.00	.096	.310	.487	.590	.683	.745	.815	.875	.935	
					h_3					
.0	-.024	-.170	-.533	-.780	-.783	0.592	1.000	1.000	.294	
.25	-.155	-.400	-.729	-.745	-.352	.553	1.000	.990	.095	
.50	-.209	-.230	-.108	.150	.486	.587	.525	.380	-.466	-.864
.75	.105	.190	.280	.360	.416	.256	-.228	-.500	-.722	
1.00	-.256	-.600	-.844	-.930	-.950	-.938	-.850	-.710	-.729	

TABLE 2

CHORDWISE DERIVATIVE OF MODESHAPES

Normalized Values of $\partial h/\partial x$ at y/ℓ =

x/c	.10	.20	.30	.40	.50	.60	.70	.80	.90	1.00
					$\partial h_1/\partial x$					
0	.02	.01	.04	.10	.33	1.74	1.77	1.80	1.70	
.25	.02	.06	.12	.29	.69	1.17	1.22	1.20	1.10	
.50	.03	.16	.34	.58	.92	.95	.96	.90	.80	
.75	.10	.24	.44	.62	.70	.81	.83	.80	.90	
1.00	.21	.25	.29	.33	.30	.39	.55	.60	1.10	
					$\partial h_2/\partial x$					
0	-.02	-.45	-1.72	-2.68	-1.01	.50	1.05	1.25	4.00	
-25	-.18	-.45	-.93	-.72	.66	1.50	3.22	5.15	7.20	
.50	.04	.19	.64	1.47	2.63	4.58	6.65	8.05	8.80	
-75	.44	1.34	2.66	3.83	4.95	6.73	7.79	7.75	7.70	
1.00	.62	2.36	4.33	6.17	7.32	5.88	5.39	5.25	5.50	
					$\partial h_3/\partial x$					
0	-.75	-2.15	-3.45	-2.63	+1.82	+17.50	+3.17	+5.80	-.72	
.25	-.41	--.15	+1.21	+3.10	+5.08	+5.90	-3.17	-6.20	-15.20	
.50	+.58	1.48	+2.88	+3.68	+3.07	-1.99	-8.19	-14.90	-16.34	
.75	-.10	-.92	-2.10	-3.60	-5.74	-7.63	-9.17	-10.90	-5.26	
1.00	-3.10	-6.98	-10.72	-13.60	-16.11	-16.26	-7.42	+2.50	+4.70	

TABLE 3

COEFFICIENTS OF LEAST-SQUARES MODESHAPE APPROXIMATION

Subsonic Coordinates

$$h_i(\xi,\eta) = \sum_{p=0}^{3} \sum_{q=0}^{3} b_{qp}^{i} \xi^{q} \eta^{2p}$$

b_{qp} mode 1

.01539	.01422	1.50484	-3.67437
.00431	1.38883	-5.40598	14.22918
-.00216	1.93035	2.76856	-16.40708
.03949	-1.56259	-.36290	6.52124

b_{qp} mode 2

-.06001	-3.33158	-2.09701	22.31879
-.02361	-3.24789	8.75556	-64.86269
.10633	6.81498	7.88875	52.98765
.14116	2.88379	-19.12408	-8.14603

b_{qp} mode 3

.04240	-13.53513	69.81547	-122.22163
.30378	24.02449	-176.59983	444.16787
-.33282	36.73225	40.53501	-471.32141
-.36186	-51.98492	76.58353	143.28380

A. Subsonic Flow

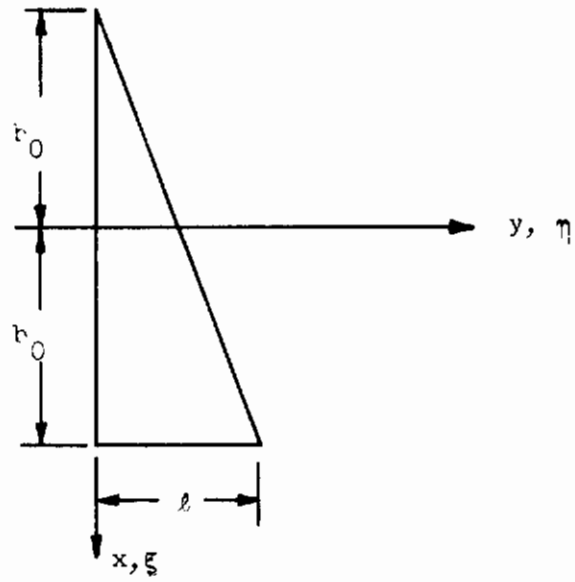

B. Supersonic Flow

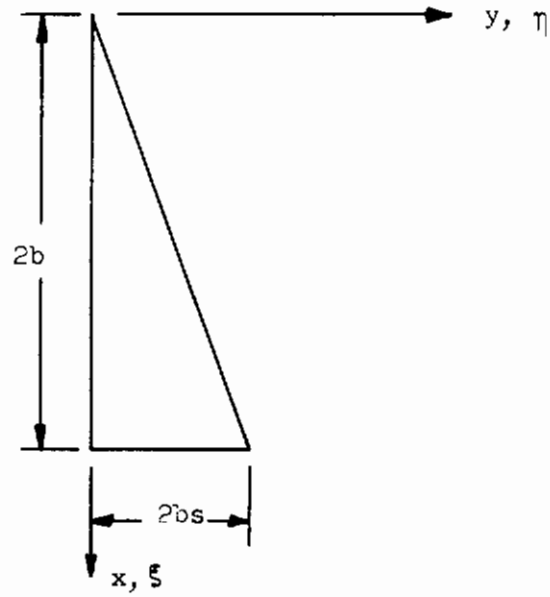

Figure 1. Coordinates and Dimensions Used in Kernel-Function Procedures

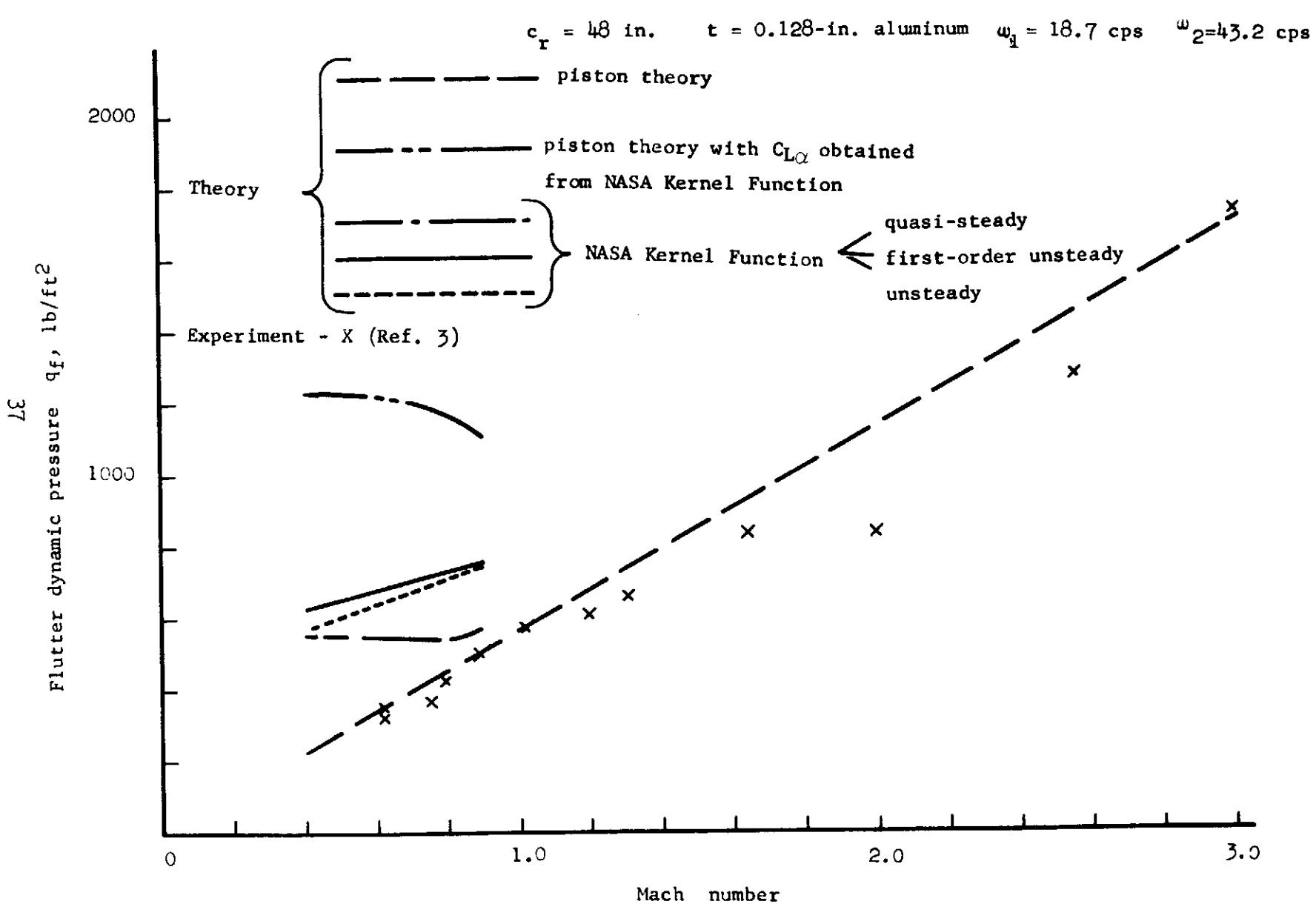

Figure 2. Comparison of Predicted Flutter Dynamic Pressures with Experiment for Thin Uniform Cantilevered 70° Delta Wing

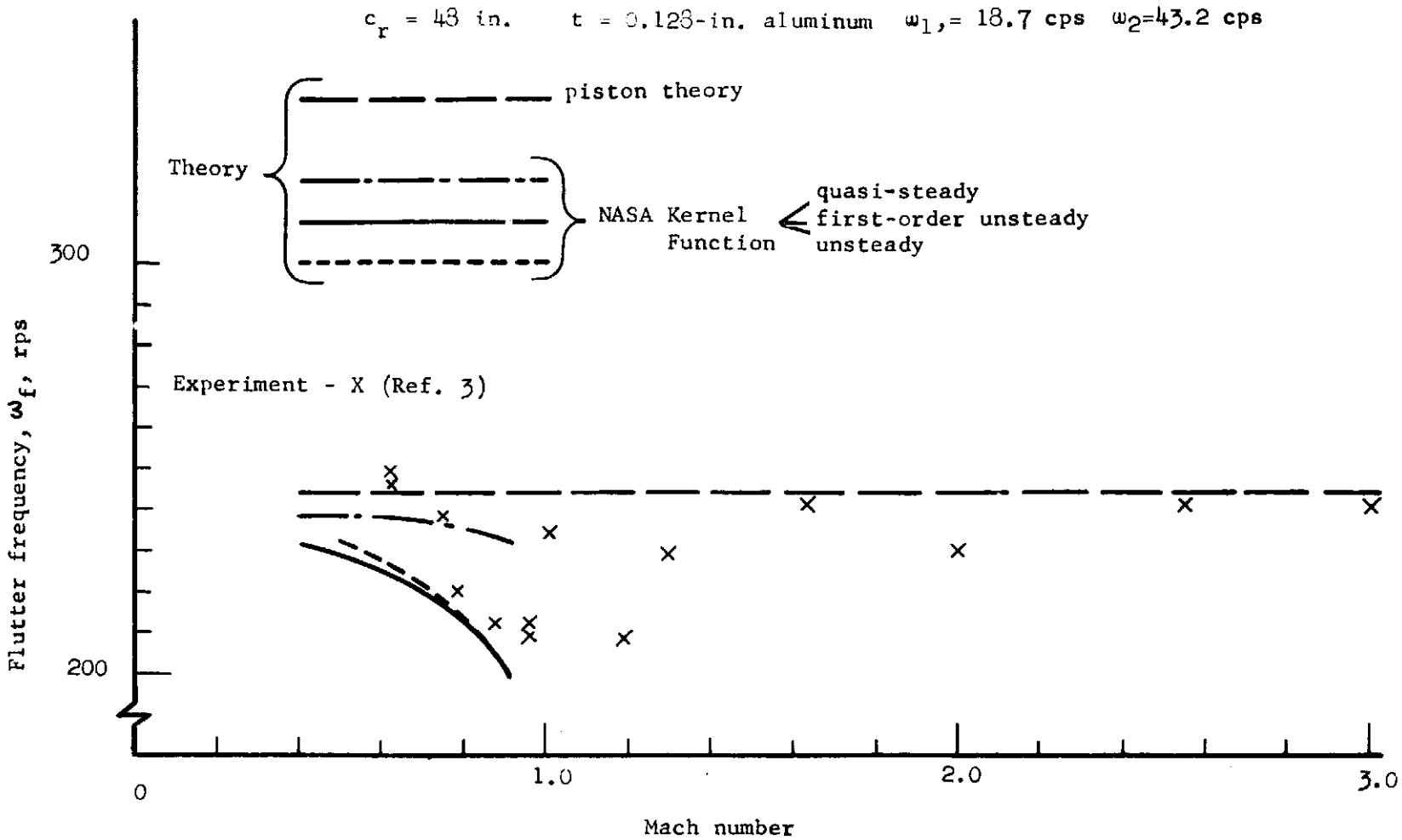

Figure 3. Comparison of Predicted Flutter Frequencies with Experiment for Thin Uniform Cantilevered 70° Delta Wing